

A Primary Study of the Variations of Vertical Radiation with the Beijing 325-m Meteorological Tower

WANG Yuesi* (王跃思), HU Bo (胡波), and LIU Guangren (刘广仁)

Institute of Atmospheric Physics, Chinese Academy of Sciences, Beijing 100029

(Received 28 May 2004; revised 1 November 2004)

ABSTRACT

The Beijing 325-m Meteorological Tower (325MT) is used to observe the vertical variation of solar radiation. Results of the experiments indicate that the automatic radiation monitoring system, including a sun tracker and data collection system, works well and all the specifications meet WMO observation standards. The measurement data show that there is a significant radiation decrease from 320 m to the surface, where the difference is only about 30 W m^{-2} on light air-pollution days, while the maximum reaches about 110 W m^{-2} when heavy pollution appears near the ground. The global UV radiation decreases on heavy air-pollution days and under poor visibility conditions, and the difference between 300 m and 8 m is larger than on clear days.

Key words: meteorological tower, vertical solar radiation variation, automatic sun tracker

1. Introduction

Direct radiation (DR) from the sun follows a beam that can be focused. DR is need for many solar-energy applications, especially for aerosol optical depth (AOD). It is necessary to know DR for the estimation of the AOD, Linke turbidity factor, and Ångström turbidity indices (Zakey et al., 2004). In this study, the data being analyzed is direct irradiance.

Diffuse radiation (SR) is that received by a horizontal surface from the above 2π solid angle, except for the solid angle of the solar disk, and the scattering DR caused by atmospheric aerosols. SR is also needed for many solar-energy applications. For example, knowledge of the SR is necessary for the estimation of the transmissivity-absorptivity product of flat-plate collectors (Veeran and Kumar, 1993), atmospheric pollution, and the effect of cloud.

There are three spectral bands of total ultraviolet radiation (TUV), namely, UV-A (400–315 nm), UV-B (315–290 nm), and UV-C (290–220 nm). Only UV-A and UV-B reach the earth's surface, while UV-C is removed by absorption through the ozone layer in the stratosphere. TUV accounts for only about 8.73% of the total solar radiation from extraterrestrial sources (Al-Aruri et al., 1988; Kirchhoff et al., 2002; Luccini

et al., 2003), however, the TUV has both beneficial and damaging effects on humans, the ecosystem, animals, plants and materials (Giese, 1982). High doses of TUV cause skin diseases, eye cataracts, photodecomposition, degradation of materials, and harm for many crops (Som, 1992).

The World Meteorological Organization (WMO) suggests that all members should try their best to derive the aerosol optical depth (AOD) from direct spectral solar radiation, and then estimate the atmospheric turbidity. Russian meteorologist С и ВКОБ (1968) indicated that direct solar radiation was a good index for atmospheric turbidity assessment. Although many scholars in China and in other countries have studied this subject, such investigations have been limited to ground observations so far (Gueymard, 1998; Li and Mou, 1994; Power, 2001; Qiu, 1995; Qiu et al., 1995; Wang and Wei, 1995; Zhang et al., 1998). Only a rough large-scale ground distribution of solar radiation can be obtained due to the sparse network of observation stations. Regarding the vertical observation, restricted by both technique and equipment, this study has been very hard to develop. So issues in this particular kind of investigation are very limited. Jiang and Ji (1992) took some observations in Lanzhou in 1992 with a tethered balloon to observe solar radiation at upper layers and found a significant

*E-mail: wys@dq.cern.ac.cn

difference between 600 m in relative height and the ground. They had to stop their work because there was no fixed frame which was high enough to monitor radiation at the upper layer. The Beijing 325-m Meteorological Tower (325MT) was built in an open field at its beginning; it has since been immersed into a metropolis with the development of Beijing city, and this provides an opportunity for us to study the vertical solar radiation variations with the change of urban air pollution. At present, there are few MTs in the world that can be used to carry out downtown vertical radiation and air pollution observation since most of them stand in open fields. In suburban areas there is nearly no change in the structure of the boundary layer and air quality. According to naked eye observation in the tower, it can be found that, under suitable conditions of atmospheric stratification, the whole city is almost submerged in fog due to the air pollution, except for the tips of high-rise buildings (usually above 100 m). This unusual phenomenon urges us to design an experiment for the measurement of the vertical solar radiation differences from 320 m to the ground.

Concentrated studies of DR, SR, and TUVR, and especially their gradients, have been very rare in Beijing city, so studying them is very important and necessary. In order to characterize DR, SR, and TUVR gradients in Beijing, an observation system was established.

This paper introduces the observation system and presents the primary results of the experiment. The vertical variation of solar radiation was remarkable below 325 m in height during the period of heavy air pollution from October 2001 to March 2002. It is worth making further research to explore the relations among radiation components, aerosols, organic compounds and greenhouse gases under different weather conditions.

2. Instruments and Experimental methods

2.1 Instruments

The observation system is composed of two parts: hardware and software. The software is responsible for hardware control, data collection, and data storage (see Fig. 1). In order to avoid interfering with each other, the hardware control and data collection run independently.

Observation equipment is installed at the levels of 8 m, 140 m, and 320 m in relative height above the ground on the 325MT. Furthermore, a set of instruments identical with that at the 8-m level is installed on the rooftop of a two-floor building (10 m) nearby the 325MT for the correction of possible errors caused by the 325MT tower body. The DR, SR, and TUVR

are observed at each layer. The TUVR is controlled particularly by one PC and the other instruments are controlled by another one.

DR was measured using a direct radiometer (TBS-2) (Junzhou, China). SR was measured using global radiometers (TBQ-2) (Jinzhou, China). TUVR was measured using CUV3 radiometers (USA). DR measurements have an estimated experimental error of 1%, and SR measurements have an estimated experimental error of 3%, while the TUVR sensor has a relative error of less than 2%. All radiation values were measured at one-minute intervals, and hourly values were obtained by integrating them.

The direct radiometers were calibrated against a standard DR radiometer; the global radiometers were calibrated against a reference pyranometer, which is calibrated by a standard pyrhelimeter; and the CUV3 radiometers were calibrated against a reference radiometer. All this calibration work was done on the rooftop of the two-floor building at the beginning and at the end of the data collection.

2.2 Observation method

2.2.1 Direction Radiation

At present, the main difficulty for the DR measurement in China is how to improve the tracking accuracy for the sun. The main disadvantage of the tracker, which usually works in equator mode, is unable to run fully automatically. Manual adjustment is required everyday but this is impossible on the 325MT, especially on cloudy days. There are a few 2D high-accuracy, PC-controlled sun trackers in France, Japan and the U.S.A. But are difficult for popular adoption in China. We designed a much cheaper sun tracker to be used on the tower, to be driven by a commercial electronic stepper motor. In addition, a remote-transmission interface and controlling software were developed for linking the PC to the motor over cables about 1000 m long. we call this 2-D high-accuracy automatic sun tracker IAP/CERN-1. The maximum possible position-error of IAP/CERN-1 is about $\pm 0.2 \text{ d}^{-1}$ (with no diurnal accumulative effect). This sun tracker can not only ensure that the DR radiometer measures the solar DR accurately, but also ensures that the global radiometer measures the solar SR accurately when the sunshine is automatically shielded with a shadow ring. It is not only much cheaper than equivalent quality sun trackers in the world, but also credible, stable, and easily maintained.

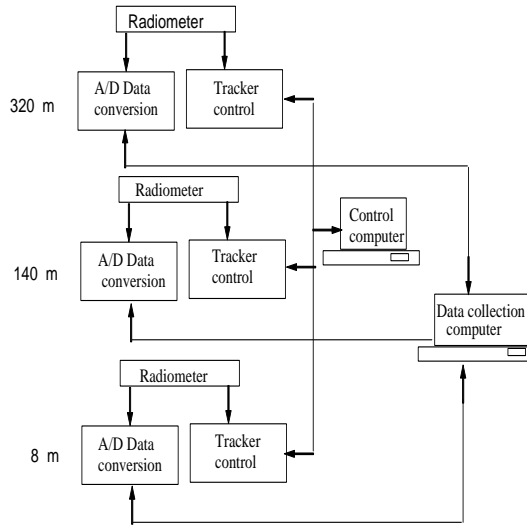


Fig. 1. Observation system of vertical solar radiation.

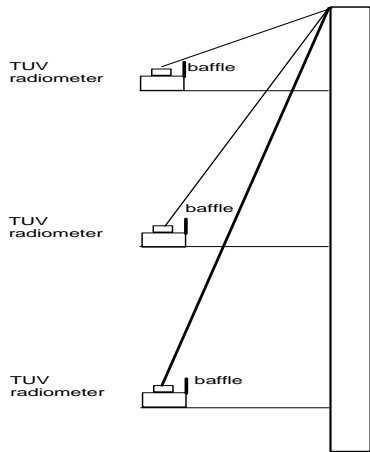


Fig. 2. Tower body effects on the TUV radiometers.

2.2.2 Diffuse Radiation and Global Radiation

SR is measured with a global radiometer in a sun tracker with a sun-shielded device. The Global Radiation (GR) is calculated with the equation

$$R_G = R_S + R_D \sin(h)$$

where R_G is global radiation, R_S is diffused radiation, R_D is direct radiation, and h is the solar elevation angle.

2.2.3 Total Ultraviolet Radiation

Because the amount of scattered radiation in the ultraviolet band is the majority of sky-scattered radiation (the maximum value of scattering ultraviolet can be 80% or more of TUVR), the shadow effect caused by the tower body on the measurement of the ultraviolet radiometers installed at different heights must

be taken into account. From the top to the bottom, each section of the tower body has different effects on the ultraviolet radiometer due to the different solid angles. There are three 3.7-m long arms for the installation of the radiometers. Three identical baffles, designed according to the maximum shadow effect near the ground, were pre-installed on the northward side of the radiometers, respectively, in order to reduce the effect and to keep it constant at different levels (See Fig. 2).

In order to correct the error of TUVR that was caused by the MT, a series of comparison measurements of TUVR radiometers were carried out on the rooftop of the two-floor building in advance with baffle and without baffle respectively.

2.3 Tracker control and software

The structure of the tracker is shown in Fig. 3. The control signals are sent by a computer indoors through the parallel port to the output interfaces. This interface sends pluse signals for driving the electrical stepper motor to the remote control input interface through an 8-line cable, which then sends positive and negative turn signals for both horizontal and pitching directions to the motor. The motor is driven by a 24V direct current (DC) power supply and another 5VDC is needed for the I/O interface. There are two photoelectric reposition switches in the tracker for the horizontal and pitching direction controls respectively, which can cause the device to stop automatically when it turns to direct north or horizontal. The sun track calculation is based on the chronometer technique, which enables the program to calculate the solar track without accumulative error. At the same time in the calculation method, the 365.2422-d cycle of the sun and the correction of atmosphere refraction, which can reach 0.5° under low solar elevation angles, are taken into account. There are two versions of the software. One works in DOS and is programmed in Quick Basic,

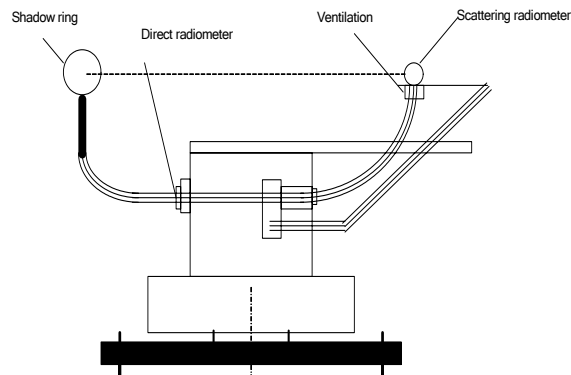


Fig. 3. Sun tracker.

and the other works in Win9X or Win2000 programmed in Visual Basic or Visual C++. The parameters needed for input at the beginning are only the longitude and latitude of the site. Then the solar position at every minute will be calculated by the program automatically and converted to the number of steps required by the electrical stepper motor in the two directions for controlling the tracker.

All the information is displayed on a monitor, including: the real-time solar azimuth angle, solar zenith angle, Beijing standard time, UTC, local time, azimuth, orientation, rotary step, elevation angle and its rotary step and total steps made when the program is running. The data are saved every minute in files named according to the date in order to check them conveniently. The tracker will reposition automatically when the solar elevation angle calculated by the PC is below the horizon, and the original position of the tracker is defined as when the light axis of the direct radiometer lies in the horizontal and the sunshine aperture points north simultaneously. When the solar elevation angle calculated by the PC is above horizon, the tracker will begin a new day's work. The tracker can work continuously without need of manual adjustment. Because the program calculates the date and time of the solar track according to the date and time of the computer, the clock of the computer needs to be adjusted before operation. However, if the time of the clock is inaccurate, the program can also correct it. The GPS (Global Positioning System) can be used for calibrating the computer time if necessary.

2.4 Data collection

Besides the instruments for radiation measurements, there is a variety of equipment installed on several platforms on the 325MT that form a very complex electromagnetic environment. In order to avoid the electromagnetic interference caused by the various instruments, industrialized products developed by the Yanhua Corporation (Taiwan) are used for data collection and system controlling. The standard RS-485 line data transfer model adopted in the system makes the remote data access possible. Equipment boxes are fixed on each platform. Three kinds of ADAM4000 (Advantech Data Acquisition Module) modules are installed in each box, viz. A/D conversion module ADAM4018, temperature measurement module ADAM4013 and on/off transformation module ADAM4050. The precision of the data transfer of ADAM4018 is 16-bit with a $1\text{-}\mu\text{V}$ resolution. The resolution of ADAM4013 is 0.1° . The ADAM4050, with 8 I/O switches, can be used for controlling circuits, fans, and system switches.

The controlling program is self-designed based on the GENIE software package developed by the Yuan-

hua Corporation. Measurement data is stored in a text file each hour, which can be processed with Microsoft Excel conveniently.

3. Calibration of the radiometer

3.1 Accuracy of the radiometer

To determine the difference in radiation among different positions within the vertical scope of 320 m is very difficult since the distance of 320 m is just the same as a single point compared to the distance between the sun and the earth. In dry and clear atmosphere conditions, there is no significant discrepancy in solar radiation among the different layers. In common polluted atmosphere conditions, the discrepancy in solar radiation among the different layers is also not very large. It is not easy to observe a radiation gradient within 320 m with common radiometers that lack precision, so radiometers with high accuracy are required for the observation system. The accuracies of the radiometers used in the experiment are as follows: the DR radiometer is about 1%, the TUVR radiometer is about 2%, and the global radiometer is about 3%. In addition, a calibration system that meets the WMO calibration standards was used to calibrate these radiometers.

3.2 The calibration method and the results of the TUVR radiometer

TUVR radiometer No. 427 is used as a TUVR standard apparatus in the experiment. Figure 4a shows observation results of the TUVR measured by No. 428, No. 488, and No. 490 in comparison with No. 427. After this calibration, baffles were installed on the northward side of the cross arm used for the TUVR radiometers, and the observation results are shown in Fig. 4b. The correct compensation for the observation data has been done. Compared to No. 427, the mean values of No. 428, No. 448, and No. 490 are larger by about 0.4%, 0.3%, and 0.2% respectively (the data have been corrected before analysis). This discrepancy is acceptable within the amount allowed by the instrument accuracy.

3.3 Comparison of DR

Figure 5 shows the results of DR measured by DR radiometers No. 02 and No. 03 compared to standard DR radiometer ZB. DR radiometer No. 02 is installed on one tracker, while No. 03 and ZB are installed on another one. They are all on the same roof of the two-floor building. The distance between these two trackers is 4 m. The measured data of ZB and No. 03 are collected in one data collection and the results of No. 02 are saved in another data collection.

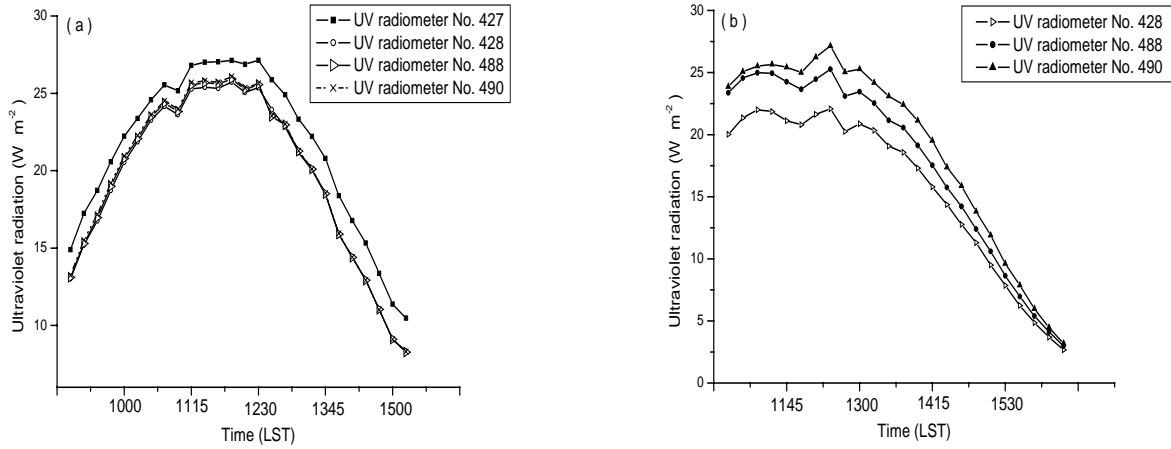


Fig. 4. Comparison of TUVR measured by No. 428, No. 488, No. 490 and standard radiometer No. 427 (a) without baffles, (b) with a baffle on the northward side of the radiometer.

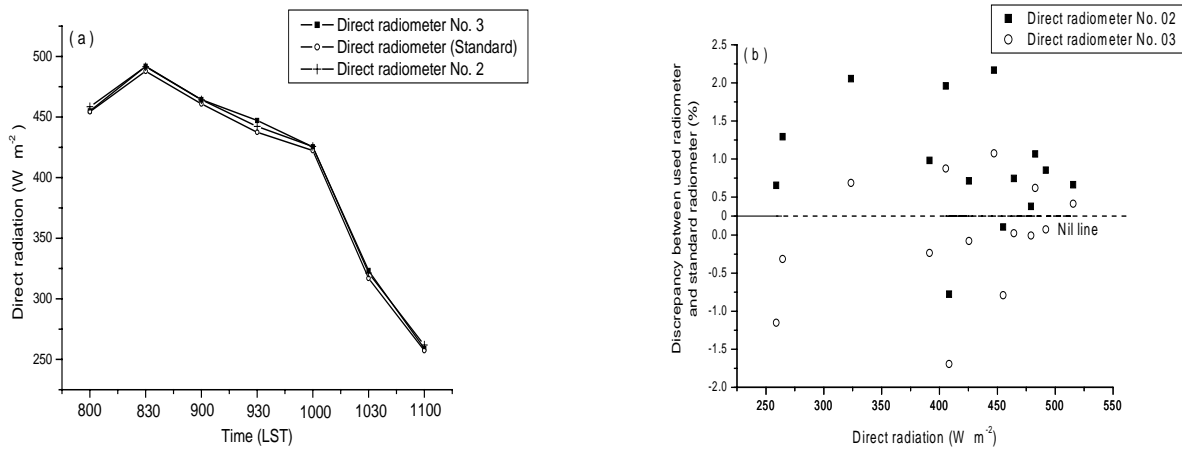


Fig. 5. (a) Comparison of DR measured by No. 02, No. 03 and standard DR radiometer ZB, (b) the discrepancy of DR measured by DR radiometers No. 02 and No. 03 with respect to standard radiometer ZB.

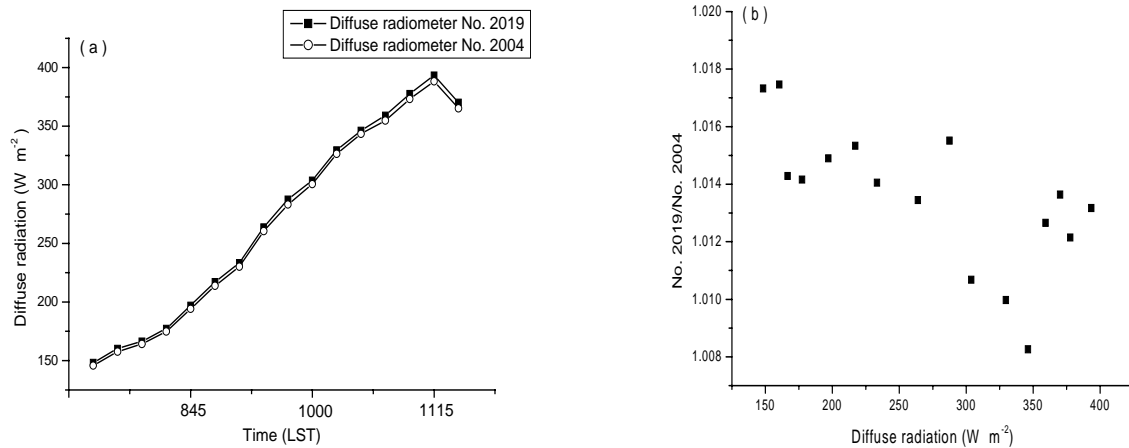


Fig. 6. (a) Comparison of SR measured by SR radiometers No. 2019 and No. 2004, (b) the ratio of SR measured by SR radiometers No. 2019 and No. 2004.

Analyses of the tracks of the sun tracker show that it tracks the sun well. From the measured data, the values of No. 03 are always higher than those of No. 02. The discrepancy between these two radiometers is only about 2%.

3.4 Comparison of SR

The SR radiometer No. 2019 is installed on one tracker and No. 2004 is installed on another one on the roof of two-floor building. As Fig. 6 shows, the variation of the No. 2019 measured value is similar to that of No. 2004 but the former is always higher than the latter. The maximum, minimum, and average discrepancy between these two radiometers is about 1.9%, 0.7%, and 1.3% respectively. This meets the experimental precision requirements.

4. Preliminary analyses of the observation data

The vertical radiation observation system was established in October 2001. It can not only measure TUVR at 8 m, 140 m, and 320 m, but also DR and SR at 8 m and 320 m. All these data are collected once per minute.

4.1 Difference of TUVR

The variations of TUVR at 8 m, 140 m, and 320 m are shown in Fig. 7. October 28 is a sunny day after rain accompanied by 4-grade wind and fine visibility. October 29 is sunny and without wind but the visibility is poor. Comparing the observed data of October 28 and 29 the figures show that TUVR and its variation range both vary from day to day. On a sunny day and fine visibility, the TUVR discrepancy is inconspicuous. On the other hand, the discrepancy is enhanced

on a poor visibility day. Figure 7a shows that values of the TUVR at 140 m are higher than at 320 m in the morning, and this reverses after noon, but the absolute discrepancy is very small (the maximum difference is about 6.67%, the average value is 3.41%).

This is only a little difference in TUVR between 320 m and 140 m on fair visibility days, but there is always a significant difference between 140 m and 8 m. On fair visibility days, there is high atmospheric transparency and low concentrations of fine particles in aerosol, so the attenuation of TUVR is smaller than that on poor visibility days (high aerosol concentration and lower atmospheric transparency). Beyond this, the influence of ozone on TUVR should be considered in a future study.

4.2 The differences of the DR and SR between 325 m and 8 m

The results of the direct radiation on sunny and fair visibility days are shown in Fig. 8. The average discrepancy between 320 m and 8 m is 42 W m^{-2} {the maximum difference ratio [which is calculated by this equation: $\text{difference ratio} = (\text{Value}_{320} - \text{Value}_8) / \text{Value}_{320} \times 100\%$] is 13%, and the average ratio is 4.89%}. The results on heavy air pollution days are shown on the right panel of Figure 9. The average discrepancy of DR between 320 m and 8 m is about 51 W m^{-2} (the maximum difference ratio is 27%, and the average ratio is 10%). On dust storm days, the discrepancy of DR is very small due to the uniformity of the atmosphere. The variation of SR shows an opposite trend compared to that of the direct radiation. There is a large difference ratio on sunny days (average difference ratio is 2%), and a little difference on dust storm days (average difference ratio is 0.41%). These differences may

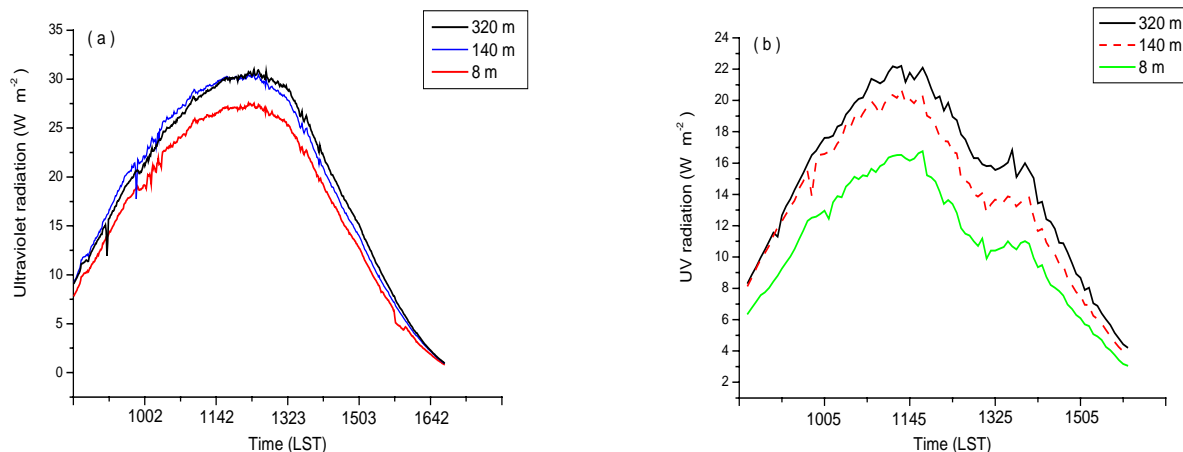


Fig. 7. The vertical variation of total UV radiation: (a) 28 October 2001; (b) 29 October 2001.

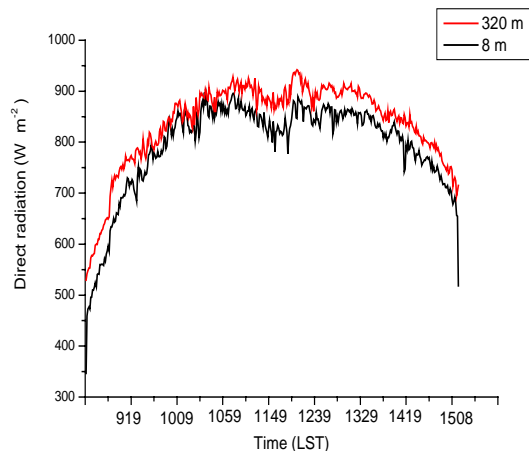


Fig. 8. The vertical variation of DR (28 January 2002).

be caused by pollutants and the variation of atmospheric conditions. The relationships between the radiation, pollution and vapor, etc., should be studied in the future.

4.3 The daily attenuation variations of DR and TUVR

The monthly average vertical attenuations of the DR and TUVR in winter are presented in Figs. 10 and 11. These figures illustrate that the attenuation ratio variations of the DR in the three winter months are similar and appear in a hyperbolic form. The maximum attenuation ratio appears in the morning and the minimum attenuation ratio appears at noon with a variation range from 36.9% to 10.8%. In the afternoon, attenuation begins to increase gradually. This variation accords with the concentration of the diurnal variation of the atmospheric aerosol concentration

(Yan et al., 2004). Usually, pollutants with high concentration exist in the Beijing atmosphere in the morning due to pollutant accumulation during the night and traffic emission in the morning. But the pollutants diffuse quickly at noon with the stronger convection as the temperature increases. The pollutant concentration then reaches its minimum and the attenuation effect of the pollutants on the DR is also weakest. The inversion layer appears again with the fading of the solar radiation in the late afternoon, and the attenuation effect increases again as pollutants accumulate in the boundary layer.

Figure 11 shows that the gradient variation of the TUVR exists at each layer. The attenuation value of the lower layer is always higher than that of the upper layer. The monthly average vertical attenuation of the TUVR appears in a hyperbolic form. The maximum attenuation ratio appears in the morning and afternoon and the minimum attenuation ratio appears at noon with a variation range from 0.2 to 0.7 in the lower layer and 0.05 to 0.45 in the upper layer. In the afternoon, the attenuation begins to increase gradually. The appearance of the minimum attenuation ratio of the lower layer occurs earlier than that of the upper layer. This variation type is caused by the concentration variation of atmospheric aerosols and the vertical distribution of aerosol concentration. The attenuation value of TUVR is mainly dependent on the fine aerosol concentration in the atmosphere. The backscattering ratio of aerosols depends on the concentration of fine aerosol particles. The higher concentration of fine aerosols causes a stronger backscattering ratio, so the backscattering value of TUVR is large. In the morning, the atmosphere is controlled by the inversion layer, and the atmospheric diffusion is low in this condition;

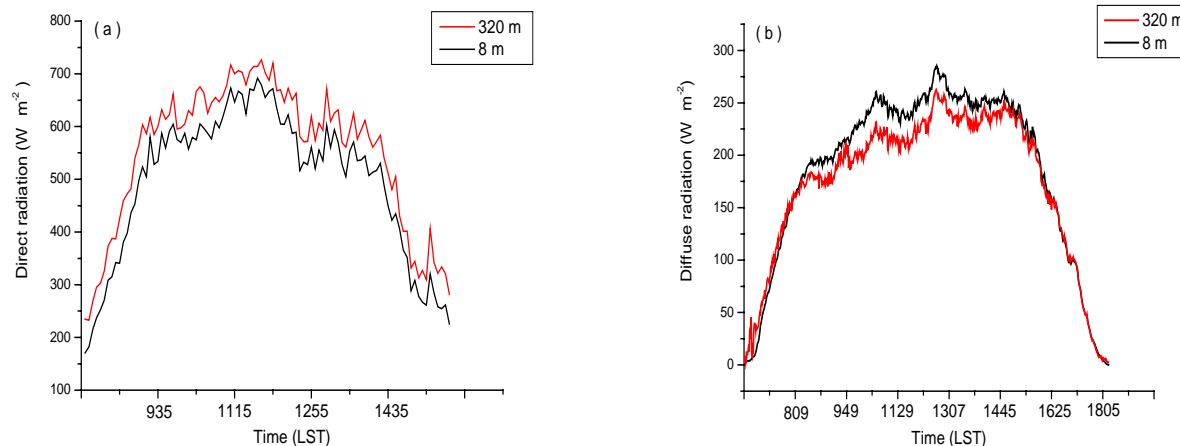


Fig. 9. (a) The vertical variation of solar radiation of DR under dust storm conditions (16 March 2002). (b) The vertical variation of SR under dust storm conditions (16 March 2002).

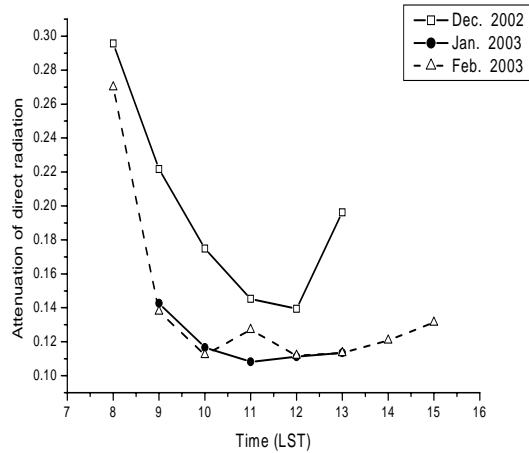


Fig. 10. The monthly average attenuation of DR (in winter).

and when we add up the traffic emission in the morning and the pollutant accumulation during the night, the concentration of fine aerosols becomes higher in the morning. But the pollutants diffuse quickly at noon with the stronger convection as the temperature increases. The pollutant concentration reaches its minimum and the attenuation effect of the pollutants on the TUVR is weak. The inversion layer appears again with the fading of the solar radiation in the late afternoon, and the attenuation effect increases again as pollutants accumulate in the boundary layer. The vertical distribution of aerosols decreases with increasing height, so the backscattering ratio of TUVR is higher in the lower layer than in the upper layer.

Although the variation of aerosol concentration is regarded as a main reason causing the decline of solar radiation, the effects of water vapor and ozone on TUVR also need to be taken into account. In this paper, the correctness of the work is restricted by limits in the observational data. Better work should be strived for in future work.

5. Conclusions

Results show that the automatic radiation monitoring system works reliably with high accuracy and sensitivity.

(1) The observation system established here is steady and reliable. It is suitable for observing the vertical variation of radiation from the 325MT. The sun tracker is reliable and accurate, and the precision of this type of sun tracker is harmonious with the precision required for the DR observation system.

(2) This is only a little difference in TUVR between 320 m and 140 m on fair visibility days, but there is always a significant difference between 140 m and 8 m.

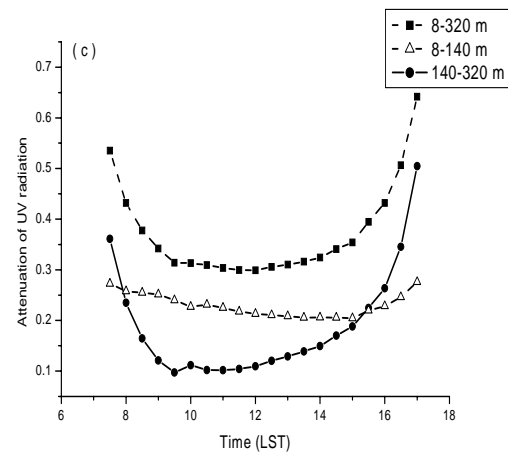
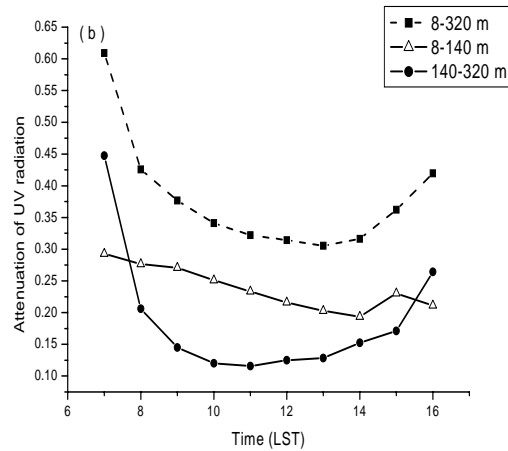
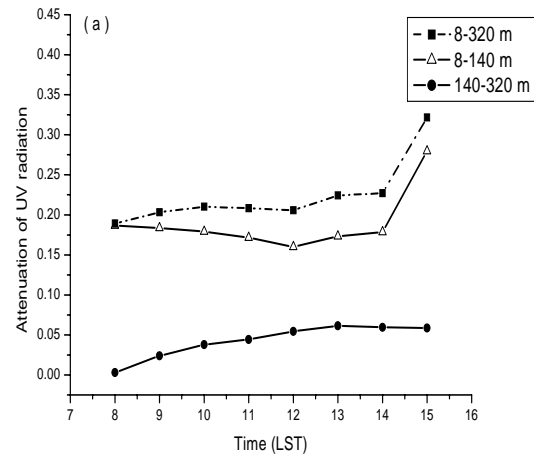


Fig. 11. The monthly average attenuation of the TUVR (in winter) (a) December 2002, (b) January 2003, (c) February 2003.

(3) The average discrepancy of DR between 320 m and 8 m is smaller on fair visibility days than on pollution days. The average discrepancy of DR between 320 m and 8 m on dust storm days is very small due

to the uniformity of the atmosphere. The variation of SR shows an opposite trend compared to DR.

(4) The attenuation ratio variations of the DR in the three winter months are similar and appear in a hyperbolic form. The maximum attenuation ratio appears in the morning, the minimum attenuation ratio appears at noon, and in the afternoon the attenuation begins to increase gradually.

(5) The variations of the TUVR's diurnal attenuation ratio follow a hyperbolic law. Large attenuation values appear in the morning and at dusk, and smaller ones at noon. In the vertical, the variation of the TUVR attenuation in the lower layer is higher than that in the upper layer; the vertical distribution of aerosol concentration causes this variation rule of TUVR.

The observation system and sun tracker should be standardized in the future. Further models should be developed for radiation vertical distribution and aerosol optical depth.

Acknowledgments. This work was supported by the National Natural Science Foundation of China Grant No. 40222202 and approved by Grant No. KZCX1-SW-01. The authors are grateful to the referees for their comments and suggestions that improved the presentation of the results.

REFERENCES

- Al-Aruri, S., M. Rasas, S. N. Al-Jamal, 1988: An assessment of global ultraviolet radiation in the range (0.290–385 μm) in Kuwait. *Solar Energy*, **41**(2), 159–162.
- С и в к о в, С. И., 1968: М е т о д ы р а с ч ё т а х а р а к т е р и с т и к с о л н е ч н о й р а д и а ц и и, -Л. Г и д р о м е т е о и з д а т .
- Giese, A. C., 1982: *living with our Sun's Ultraviolet Rays*. Plenum Press, New York.
- Gueymard, C., 1998: Turbidity determination from broadband irradiance measurements: A detailed multicoefficient approach. *J. Appl. Meteor.*, **37**, 414–435.
- Jiang Hao, and Ji Guoliang, 1995: The radiation condition of atmosphere polluted over Lanzhou in winter of 1992. *Plateau Meteorology*, **14**, 151–156. (in Chinese)
- Kirchoff, V. W., A. Silva, and K. Pinheiro, 2002: Wavelength dependence of aerosol optical thickness in the UV-B band. *Geophys. Res. Lett.*, **29**(12), 1620, doi: 10.1029/2001.
- Li Aizhen, and Mou Jiwang, 1994: Space change of urban radiation in fine day. *Urban Environment and Urban Ecology*, **7**, 26–30. (in Chinese)
- Luccini, E., A. Cede, and B. Mayer, 2003: The effect of clouds on UV and total irradiance at Paradise Bay, Antarctic Peninsula, from a summer 2000 campaign. *Theor. Appl. Climatol.*, **75**, 105–116.
- Power, H. C., 2001: Estimating atmospheric turbidity from climate data. *Atmospheric Environment*, **35**, 125–134.
- Qiu Jinhuan, 1995: A new method of determining atmospheric aerosol optical depth from the whole-spectral solar direct radiation. Part I: Theory. *Scientia Atmospherica Sinica*, **19**, 385–394. (in Chinese)
- Qiu Jinhuan, Yang Jingmei, and Pan Jidong, 1995: A new method of determining atmospheric aerosol optical depth from the whole-spectral solar direct radiation. Part II: Experimental study. *Scientia Atmospherica Sinica*, **19**, 586–596. (in Chinese)
- Som, A. K., 1992: Solar UV-B radiation measurements over Bahrain. *Renewable Energy*, **2**(1), 93–98.
- Veeran, P. K., and S. Kumar, 1993: Diffuse radiation on a horizontal surface at Madras. *Renewable Energy*, **3**(8), 931–934.
- Wang Raoqi, and Wei Zhigang, 1995: The direct solar radiation and the atmospheric transparency over Hexi region. *Acta Meteorologica Sinica*, **53**(3), 375–379. (in Chinese)
- Yan Fenqi, Hu Huanling, Wu Yonghua, Fan Aiyuan, and Yu Tong, 2004: Variation of aerosol parameters in the summer and winter in Beijing. *Research of Environment Sciences*, **17**(1), 30–33. (in Chinese)
- Zkey, A. S., M. M. Abdelwahab, and P. A. Makar, 2004: Atmospheric turbidity over Egypt. *Atmospheric Environment*, **38**, 1579–1591.
- Zhang Yiping, Li Yulin, and Zhang Qingping, 1998: On the characteristics of radiation in polluted atmosphere under different weather conditions in the region of Kunming city. *Resources and Environment in the Yangtze Basin*, **7**(1), 63–69. (in Chinese)